research communications

Synthesis, crystal structure and thermal properties of bis(acetonitrile-κN)bis(3-bromopyridine-κN)bis(thiocyanato-κN)cobalt(II)

Christoph Krebs, Inke Jess and Christian Näther*

Institute of Inorganic Chemistry, University of Kiel, Max-Eyth-Str. 2, 24118 Kiel, Germany. *Correspondence e-mail: cnaether@ac.uni-kiel.de

Single crystals of the title compound, $[Co(NCS)_2(C_5H_4BrN)_2(C_2H_3N)_2]$, were obtained by the reaction of $Co(NCS)_2$ with 3-bromopyridine in acetonitrile. The Co^{II} cations lie on crystallographic inversion centers and are coordinated by two N-bonded thiocyanate anions, two 3-bromopyridine and two acetonitrile ligands thereby forming slightly distorted CoN_6 octahedra. In the crystal, these complexes are linked by C—H···S and C—H···N hydrogen bonds into a three-dimensional network. In the direction of the crystallographic b-axis, the complexes are arranged into columns with neighboring 3-bromopyridine ligands stacked onto each other, indicating π–π interactions. The CN stretching vibration of the thiocyanate anions is observed at 2066 cm^{-1}, in agreement with the presence of only N-bonded anionic ligands. TG-DTA measurements reveal that in the first mass loss the acetonitrile ligands are removed and that in the second step, half of a 3-bromopyridine ligand is lost, leading to the formation of a polymeric compound with the composition $[(Co(NCS)_2)_2(C_5H_4BrN)_3]_n$ already reported in the literature.

1. Chemical context

Coordination compounds based on thiocyanate anions show a large structural variability, which to some extend can be traced back to the versatile coordination behavior of this ligand and this is surely one reason why, for example, many isomeric compounds are known (Jochim *et al.*, 2020a; Böhme *et al.*, 2020; Neumann *et al.*, 2018; Werner *et al.*, 2015a). Moreover, in bridging thiocyanate anions a reasonable magnetic exchange is present, which can lead to compounds with a variety of magnetic properties (Palion-Gazda *et al.*, 2015; Mekuimemba *et al.*, 2018). In this context, compounds based on Co^{II} cations are of special interest, not only because they can show anti-ferromagnetic or ferromagnetic ordering but as also for the strong magnetic anisotropy and slow relaxation of the magnetization indicative of single-chain-magnet behavior that can be observed (Böhme *et al.*, 2019; Switlicka *et al.*, 2020; Werner *et al.*, 2014; Shurdha *et al.*, 2013; Prananto *et al.*, 2017; Mautner *et al.*, 2018). The latter is observable in linear chain compounds, in which the Co^{II} cations are octahedrally coordinated in an all *trans*-configuration and linked by pairs of thiocyanate anions (Werner *et al.*, 2015b; Mautner *et al.*, 2018; Rams *et al.*, 2020). This is the most common structural motif for such compounds, although corrugated chains or layers are also known (Chen *et al.*, 2002; Wang *et al.*, 2005; Jin *et al.*, 2007; Shi *et al.*, 2007; Yang *et al.*, 2007; Suckert *et al.*, 2016). All of these are reasons why we became interested in this class of compounds in order to study the influence of a chemical and a
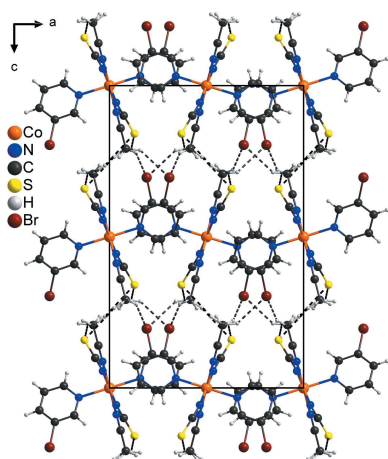
structural modification on their magnetic properties (Wöhlert *et al.*, 2014; Neumann *et al.*, 2019; Rams *et al.*, 2017*a*,*b*, 2020; Jochim *et al.*, 2020*b*; Ceglarska *et al.*, 2021).

In this context we have reported on the synthesis, crystal structures and magnetic properties of coordination compounds based on Co(NCS)₂ and 3-bromopyridine (C₅H₄BrN) as a ligand (Böhme *et al.*, 2022). During these investigations, we obtained discrete complexes with the composition Co(NCS)₂(3-bromopyridine)₄, Co(NCS)₂(3-bromopyridine)₂(H₂O)₂ and Co(NCS)₂(3-bromopyridine)₂(MeOH)₂ that lose the ligands stepwise upon heating, leading to the formation of compounds with the composition [(Co(NCS)₂)₂(3-bromopyridine)₃]ₙ and [Co(NCS)₂(3-bromopyridine)₂]ₙ, in which the Co cations are linked into chains by pairs of μ-1,3 bridging thiocyanate anions. In the latter compound, each of the Co^{II} cations is octahedrally coordinated, whereas in the former an alternating octahedral and square-planar coordination is observed, which is very rare for thiocyanate compounds and had never been observed previously with Co(NCS)₂. Later it was found that the compound with the mixed coordination can also be obtained from solution, which is impossible for the other compound with only an octahedral coordination. Unfortunately, the synthesis of the latter is difficult to achieve because all thermogravimetric curves are not well resolved and thermal annealing of the discrete complexes can lead to pure samples, but sometimes this is not the case. Therefore, we looked for other precursors that might show a similar reactivity and that might lead more easily to pure samples. In the course of these investigations, we obtained crystals of the title compound by the reaction of Co(NCS)₂, 3-bromopyridine and acetonitrile. The CN stretching vibration of the thiocyanate anions is observed at 2066 cm^{-1} in the IR spectrum, which points to the presence of terminal N-bonded thiocyanate anions (Fig. S1). Single-crystal structure analysis proved that the structure consists of discrete complexes with the composition Co(NCS)₂(3-bromopyridine)₂(acetonitrile)₂ and a comparison of the experimental XRPD pattern with that calculated from single-crystal data reveals that a pure phase has been obtained (Fig. S2). Therefore, this compound might be a suitable precursor for the synthesis of compounds, in which the Co^{II} cations are linked by μ-1,3 bridging thiocyanate anions into chains.
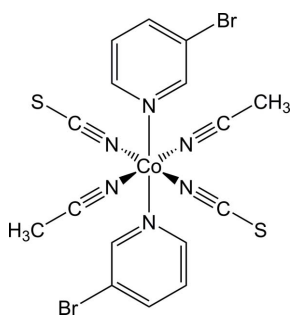
Investigations using thermogravimetry and differential thermoanalysis (TG-DTA) show several mass losses, that are each accompanied with endothermic events in the DTA curve

(Fig. S3). The experimental mass loss is in excellent agreement with that, calculated for the removal of two acetonitrile ligands ($\Delta m = 14.3\%$), whereas the values for the second and third mass loss roughly correspond to the emission of half a 3-bromopyridine ligand in each step ($\Delta m = 13.8\%$). Therefore, one can assume that in the first TG step a compound with the composition Co(NCS)₂(3-bromopyridine)₂ will form, which transforms into (Co(NCS)₂)₂(3-bromopyridine)₃ upon further heating. XRPD investigations of the residue obtained after the first mass loss reveal the formation of a compound of poor crystallinity that cannot be identified. In contrast, a comparison of the powder pattern of the residue formed after the second TG step with that calculated for [(Co(NCS)₂)₂(3-bromopyridine)₃]ₙ (Böhme *et al.*, 2022) retrieved from the literature proves that this chain compound has formed (Fig. S4).

2. Structural commentary

The asymmetric unit of the title compound consists of one crystallographically independent Co cation that is located on a center of inversion, as well as one thiocyanate anion, one 3-bromopyridine and one acetonitrile ligand in general positions (Fig. 1). The methyl H atoms of the acetonitrile ligands are disordered over two orientations rotated by about 120° and were refined using a split model. The Co^{II} cations are
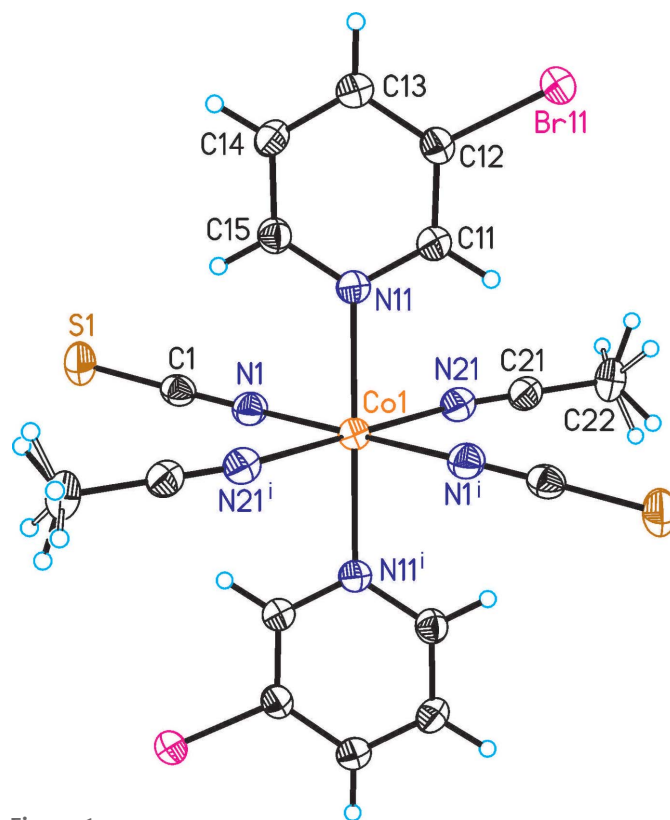

Figure 1
Crystal structure of the title compound with atom labeling and displacement ellipsoids drawn at the 50% probability level. Symmetry code: (i) −x + 1, −y + 1, −z + 1. The disorder of the methyl H atoms is shown as full and open bonds.

Table 1
Selected geometric parameters (Å, °).

Co1—N1	2.0736 (19)	Co1—N21	2.161 (2)
Co1—N11	2.1759 (19)		
N1^i—Co1—N11	90.27 (7)	N21^i—Co1—N11	90.59 (7)
N1—Co1—N11	89.73 (7)	N21—Co1—N11	89.41 (7)
N1^i—Co1—N21	84.79 (7)	Co1—N1—C1	154.96 (18)
N1—Co1—N21	95.21 (7)	Co1—N21—C21	160.05 (18)

Symmetry code: (i) $-x + 1, -y + 1, -z + 1$.

octahedrally coordinated by two symmetry-related 3-bromo-pyridine and two acetonitrile ligands as well as two terminal N-bonded thiocyanate anions into discrete complexes (Fig. 1). Bond lengths and angles correspond to literature values and from the bonding angles it is obvious that the octahedra are moderately distorted (Fig. 1 and Table 1). This is in agreement with the values for the octahedral angle variance of 10.02$°^2$ and the mean octahedral quadratic elongation of 1.0037, calculated using the method of Robinson *et al.* (1971). The six-membered rings of the 3-bromopyridine ligands coordinating to the Co^{II} cations are coplanar by symmetry.

3. Supramolecular features

In the extended structure of the title compound, the discrete complexes are linked by C—H···S and C—H···Br inter-

Table 2
Hydrogen-bond geometry (Å, °).

D—H···A	D—H	H···A	D···A	D—H···A
C11—H11···N1^i	0.95	2.60	3.109 (3)	114
C15—H15···N1	0.95	2.63	3.121 (3)	113
C22—H22A···S1^{ii}	0.98	2.98	3.947 (3)	168
C22—H22B···S1^{iii}	0.98	2.76	3.625 (3)	147
C22—H22C···Br11^{iv}	0.98	2.97	3.840 (3)	148
C22—H22F···Br11^v	0.98	2.92	3.681 (3)	135

Symmetry codes: (i) $-x + 1, -y + 1, -z + 1$; (ii) $x, -y + \frac{1}{2}, z - \frac{1}{2}$; (iii) $-x + 1, -y, -z + 1$; (iv) $x + \frac{1}{2}, y, -z + \frac{1}{2}$; (v) $-x + 1, y - \frac{1}{2}, -z + \frac{1}{2}$.

actions into a three-dimensional network (Fig. 2 and Table 2). One C—H···S angle is close to linear, whereas the other C—H···S and C—H···Br angles are much less than 180°, indicating only weak interactions (Table 2). There are additional C—H···N contacts but their bonding angles are very far from linear (Table 2). The discrete complexes are arranged in stacks that propagate along the crystallographic *b*-axis direction (Fig. 2). Within these stacks, neighboring pyridine rings are nearly coplanar with an angle between their mean planes of 10.8 (1)° and a distance between the centroids of the rings of 4.037 (1) Å, indicating very weak π–π stacking interactions (Fig. 3).

4. Database survey

Some crystal structures with thiocyanate anions and 3-bromopyridine as a coligand have already been reported in the Cambridge Structural Database (CSD version 5.42, last update November 2021; Groom *et al.*, 2016). They include [Cu(NCS)$_2$(3-bromopyridine)$_2$]$_2$, which consists of dimers, in which each Cu^{II} cation is coordinated by two 3-bromopyridine
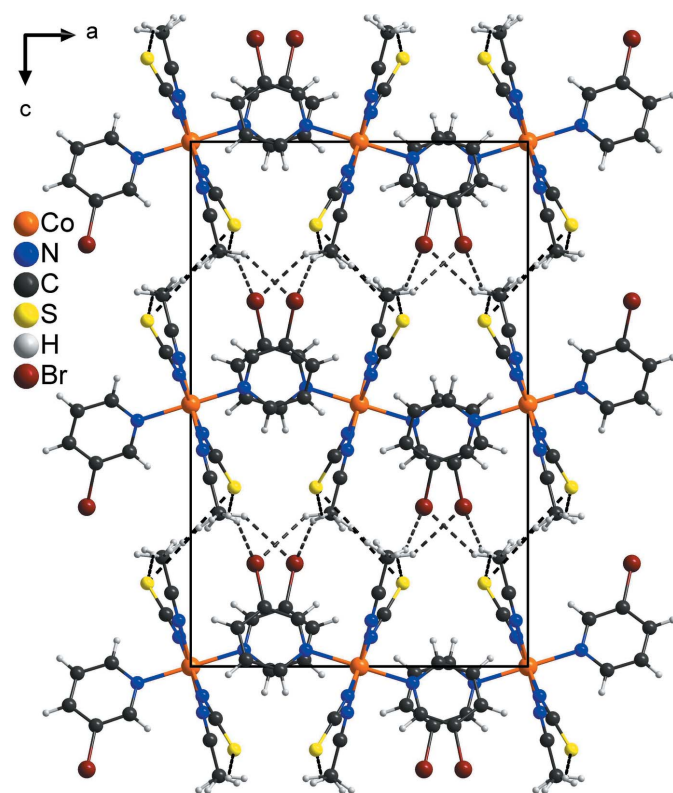

Figure 2
Crystal structure of the title compound with view along the crystallographic *b*-axis and intermolecular C—H···S and C—H···Br hydrogen bonding shown as dashed lines. Please note that the methyl H atoms of the acetonitrile ligand are disordered.
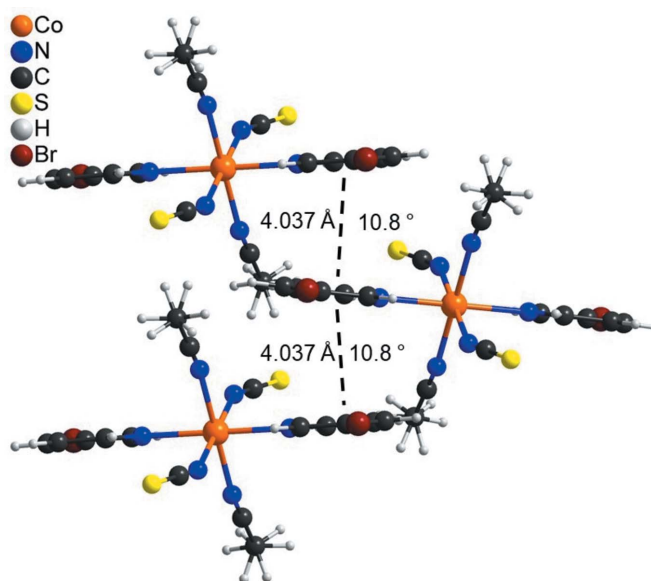

Figure 3
Crystal structure of the title compound showing the orientation of neighboring 3-bromopyridine rings. The distance between the centroids of the six-membered rings and the angles between the ring planes are shown. Please note that the methyl H atoms of the acetonitrile ligand are disordered.

Table 3
Experimental details.

Crystal data	
Chemical formula	$[Co(NCS)_2(C_5H_4BrN)_2(C_2H_3N)_2]$
M_r	573.20
Crystal system, space group	Orthorhombic, $Pbca$
Temperature (K)	100
a, b, c (Å)	13.1206 (2), 8.0606 (2), 20.4520 (4)
V (Å^3)	2163.00 (8)
Z	4
Radiation type	Cu $K\alpha$
μ (mm^{-1})	12.47
Crystal size (mm)	$0.16 \times 0.08 \times 0.02$
Data collection	
Diffractometer	XtaLAB Synergy, Dualflex, HyPix
Absorption correction	Multi-scan (*CrysAlis PRO*; Rigaku OD, 2021)
T_{min}, T_{max}	0.689, 1.000
No. of measured, independent and observed [$I > 2\sigma(I)$] reflections	10492, 2289, 2142
R_{int}	0.023
$(\sin \theta/\lambda)_{max}$ (Å^{-1})	0.634
Refinement	
$R[F^2 > 2\sigma(F^2)]$, $wR(F^2)$, S	0.027, 0.084, 1.10
No. of reflections	2289
No. of parameters	126
H-atom treatment	H-atom parameters constrained
$\Delta\rho_{max}, \Delta\rho_{min}$ (e Å^{-3})	0.38, −0.53

Computer programs: *CrysAlis PRO* (Rigaku OD, 2021), *SHELXT2014/5* (Sheldrick, 2015a), *SHELXL2016/6* (Sheldrick, 2015b), *DIAMOND* (Brandenburg & Putz, 1999) and *publCIF* (Westrip, 2010).

coligands as well as one terminal and two μ-1,3 bridging thiocyanate anions (Handy *et al.*, 2017). In CuNCS(3-bromopyridine), the copper(I) cations are tetrahedrally coordinated and linked into layers by μ-1,3 bridging thiocyanate anions (Miller *et al.*, 2011). In the second Cu^{II} compound $(CuNCS)_2(3$-bromopyridine$)_4$, the copper cations are also tetrahedrally coordinated but linked into chains by μ-1,3 bridging thiocyanate anions (Nicholas, *et al.*, 2017).

With Ni(NCS)$_2$ and 3-bromopyridine several compounds are reported, including the discrete complexes with octahedrally coordinated Ni^{II} cations Ni(NCS)$_2$(3-bromopyridine)$_4$, Ni(NCS)$_2$(3-bromopyridine)$_2$(H$_2$O)$_2$ and Ni(NCS)$_2$(3-bromopyridine)$_2$(CH$_3$OH)$_2$ (Krebs *et al.*, 2021). Also included is a compound with acetonitrile with the composition Ni(NCS)$_2$(3-bromopyridine)$_2$·CH$_3$CN, but in this structure the Ni^{II} cations are linked into corrugated chains by μ-1,3 bridging thiocyanate anions that are connected *via* intermolecular hydrogen bonding into a three-dimensional network that contains channels in which acetonitrile solvate molecules are embedded (Krebs *et al.*, 2021). Finally, when the discrete complexes are heated, a transformation into Ni(NCS)$_2$(3-bromopyridine)$_2$ is observed, in which the Ni^{II} cations are octahedrally coordinated and linked into chains by pairs of μ-1,3 bridging thiocyanate anions (Krebs *et al.*, 2021). The latter compound is isotypic to its Co^{II} analog reported recently (Böhme *et al.*, 2022).

With diamagnetic cations, four structures are reported. The compounds M(NCS)$_2$(3-bromopyridine)$_4$ (M = Zn, Cd) are isotypic and consist of discrete complexes in which the metal

cations are octahedrally coordinated by four 3-bromopyridine ligands and two terminal N-bonded thiocyanate anions (Wöhlert *et al.*, 2013). Upon heating, half of the 3-bromopyridine ligands are removed and a transformation into compounds of the composition M(NCS)$_2$(3-bromopyridine)$_2$ (M = Zn, Cd) is observed (Wöhlert *et al.*, 2013). The Zn compounds consist of tetrahedral complexes, whereas in the Cd compound the cations are linked by pairs of anionic ligands into chains.

5. Synthesis and crystallization

Co(NCS)$_2$ and 3-bromopyridine were purchased from Merck. All chemicals were used without further purification. After storing 0.5 mmol of Co(NCS)$_2$ (87.5 mg) and 0.5 mmol of 3-bromopyridine (48.8 µl) in 2.0 ml of acetonitrile for 3 d at room temperature, light-red single crystals of the title compound suitable for single-crystal X-ray analysis were obtained. The IR spectrum was measured using an ATI Mattson Genesis Series FTIR Spectrometer, control software *WINFIRST*, from ATI Mattson. The XRPD measurement was performed with Cu $K\alpha_1$ radiation (λ = 1.540598 Å) using a Stoe Transmission Powder Diffraction System (STADI P) equipped with a MYTHEN 1K detector and a Johansson-type Ge(111) monochromator. Thermogravimetry and differential thermoanalysis (TG–DTA) measurements were performed in a dynamic nitrogen atmosphere in Al$_2$O$_3$ crucibles using a STA-PT 1000 thermobalance from Linseis. The instrument was calibrated using standard reference materials.

6. Refinement

The C-bound H atoms were positioned with idealized geometry (methyl H atoms allowed to rotate but not to tip) and were refined isotropically with $U_{iso}(H) = 1.2U_{eq}(C)$ (1.5 for methyl H atoms) using a riding model. The H atoms of the methyl group of the acetonitrile ligand are disordered in two orientations and were refined in ratio 50:50 using a split model. Crystal data, data collection and structure refinement details are summarized in Table 3.

References

Böhme, M., Jochim, A., Rams, M., Lohmiller, T., Suckert, S., Schnegg, A., Plass, W. & Näther, C. (2020). *Inorg. Chem.* **59**, 5325–5338.
Böhme, M. & Plass, W. (2019). *Chem. Sci.* **10**, 9189–9202.
Böhme, M., Rams, M., Krebs, C., Mangelsen, S., Jess, I., Plass, W. & Näther, C. (2022). *Inorg. Chem.* **61**, 16841–16855.

research communications

Brandenburg, K. & Putz, H. (1999). *DIAMOND*. Crystal Impact GbR, Bonn, Germany.

Ceglarska, M., Böhme, M., Neumann, T., Plass, W., Näther, C. & Rams, M. (2021). *Phys. Chem. Chem. Phys.* **23**, 10281–10289.

Chen, H. & Chen, X. M. (2002). *Inorg. Chim. Acta*, **329**, 13–21.

Groom, C. R., Bruno, I. J., Lightfoot, M. P. & Ward, S. C. (2016). *Acta Cryst.* B**72**, 171–179.

Handy, J. V., Ayala, G. & Pike, R. D. (2017). *Inorg. Chim. Acta*, **456**, 64–75.

Jin, Y., Che, Y. X. & Zheng, J. M. (2007). *J. Coord. Chem.* **60**, 2067–2074.

Jochim, A., Lohmiller, T., Rams, M., Böhme, M., Ceglarska, M., Schnegg, A., Plass, W. & Näther, C. (2020a). *Inorg. Chem.* **59**, 8971–8982.

Jochim, A., Rams, M., Böhme, M., Ceglarska, M., Plass, W. & Näther, C. (2020b). *Dalton Trans.* **49**, 15310–15322.

Krebs, C., Ceglarska, M. & Näther, C. (2021). *Z. Anorg. Allg. Chem.* **647**, 552–559.

Mautner, F. A., Traber, M., Fischer, R. C., Torvisco, A., Reichmann, K., Speed, S., Vicente, R. & Massoud, S. S. (2018). *Polyhedron*, **154**, 436–442.

Mekuimemba, C. D., Conan, F., Mota, A. J., Palacios, M. A., Colacio, E. & Triki, S. (2018). *Inorg. Chem.* **57**, 2184–2192.

Miller, K. M., McCullough, S. M., Lepekhina, E. A., Thibau, I. J., Pike, R. D., Li, X., Killarney, J. P. & Patterson, H. H. (2011). *Inorg. Chem.* **50**, 7239–7249.

Neumann, C., Rams, M., Tomkowicz, Z., Jess, I. & Näther, C. (2019). *Chem. Commun.* **55**, 2652–2655.

Neumann, T., Ceglarska, M., Germann, L. S., Rams, M., Dinnebier, R. E., Suckert, S., Jess, I. & Näther, C. (2018). *Inorg. Chem.* **57**, 3305–3314.

Nicholas, A. D., Otten, B. M., Ayala, G., Hutchinson, J., Wojtas, L., Omary, M. A., Pike, R. D. & Patterson, H. H. (2017). *J. Phys. Chem.* **C121**, 25430–25439.

Palion-Gazda, J., Machura, B., Lloret, F. & Julve, M. (2015). *Cryst. Growth Des.* **15**, 2380–2388.

Prananto, Y. P., Urbatsch, A., Moubaraki, B., Murray, K. S., Turner, D. R., Deacon, G. B. & Batten, S. R. (2017). *Aust. J. Chem.* **70**, 516–528.

Rams, M., Böhme, M., Kataev, V., Krupskaya, Y., Büchner, B., Plass, W., Neumann, T., Tomkowicz, Z. & Näther, C. (2017b). *Phys. Chem. Chem. Phys.* **19**, 24534–24544.

Rams, M., Jochim, A., Böhme, M., Lohmiller, T., Ceglarska, M., Rams, M. M., Schnegg, A., Plass, W. & Näther, C. (2020). *Chem. Eur. J.* **26**, 2837–2851.

Rams, M., Tomkowicz, Z. A., Böhme, M., Plass, W., Suckert, S., Werner, J., Jess, I. & Näther, C. (2017a). *Phys. Chem. Chem. Phys.* **19**, 3232–3243.

Rigaku OD (2021). *CrysAlis PRO*. Rigaku Oxford Diffraction.

Robinson, K., Gibbs, G. V. & Ribbe, P. H. (1971). *Science*, **172**, 567–570.

Sheldrick, G. M. (2015a). *Acta Cryst.* A**71**, 3–8.

Sheldrick, G. M. (2015b). *Acta Cryst.* C**71**, 3–8.

Shi, J. M., Chen, J. N., Wu, C. J. & Ma, J. P. (2007). *J. Coord. Chem.* **60**, 2009–2013.

Shurdha, E., Moore, C. E., Rheingold, A. L., Lapidus, S. H., Stephens, P. W., Arif, A. M. & Miller, J. S. (2013). *Inorg. Chem.* **52**, 10583–10594.

Suckert, S., Rams, M., Böhme, M., Germann, L., Dinnebier, R. E., Plass, W., Werner, J. & Näther, C. (2016). *Dalton Trans.* **45**, 18190–18201.

Świtlicka, A., Machura, B., Kruszynski, R., Moliner, N., Carbonell, J. M., Cano, J., Lloret, F. & Julve, C. (2020). *Inorg. Chem. Front.* **7**, 4535–4552.

Wang, X. Y., Li, B. L., Zhu, X. & Gao, S. (2005). *Eur. J. Inorg. Chem.* pp. 3277–3286.

Werner, J., Rams, M., Tomkowicz, Z. & Näther, C. (2014). *Dalton Trans.* **43**, 17333–17342.

Werner, J., Runčevski, T., Dinnebier, R. E., Ebbinghaus, S. G., Suckert, S. & Näther, C. (2015a). *Eur. J. Inorg. Chem.* pp. 3236–3245.

Werner, J., Tomkowicz, Z., Rams, M., Ebbinghaus, S. G., Neumann, T. & Näther, C. (2015b). *Dalton Trans.* **44**, 14149–14158.

Westrip, S. P. (2010). *J. Appl. Cryst.* **43**, 920–925.

Wöhlert, S., Jess, I. & Näther, C. (2013). *Inorg. Chim. Acta*, **407**, 243–251.

Wöhlert, S., Tomkowicz, Z., Rams, M., Ebbinghaus, S. G., Fink, L., Schmidt, M. U. & Näther, C. (2014). *Inorg. Chem.* **53**, 8298–8310.

Yang, G., Zhang, Q., Zhang, X. P., Zhu, Y. & Ng, S. W. (2007). *J. Chem. Res.* pp. 384–386.

supporting information

Synthesis, crystal structure and thermal properties of bis(acetonitrile-*κN*)bis(3-bromopyridine-*κN*)bis(thiocyanato-*κN*)cobalt(II)

Christoph Krebs, Inke Jess and Christian Näther

Computing details

Data collection: *CrysAlis PRO* (Rigaku OD, 2021); cell refinement: *CrysAlis PRO* (Rigaku OD, 2021); data reduction: *CrysAlis PRO* (Rigaku OD, 2021); program(s) used to solve structure: *SHELXT2014/5* (Sheldrick, 2015a); program(s) used to refine structure: *SHELXL2016/6* (Sheldrick, 2015b); molecular graphics: *DIAMOND* (Brandenburg & Putz, 1999); software used to prepare material for publication: *publCIF* (Westrip, 2010).

Bis(acetonitrile-*κN*)bis(3-bromopyridine-*κN*)bis(thiocyanato-*κN*)cobalt(II)

Crystal data

[Co(NCS)$_2$(C$_5$H$_4$BrN)$_2$(C$_2$H$_3$N)$_2$]	D_x = 1.760 Mg m^{-3}
M_r = 573.20	Cu $K\alpha$ radiation, λ = 1.54184 Å
Orthorhombic, *Pbca*	Cell parameters from 8002 reflections
a = 13.1206 (2) Å	θ = 4.3–77.9°
b = 8.0606 (2) Å	μ = 12.47 mm^{-1}
c = 20.4520 (4) Å	T = 100 K
V = 2163.00 (8) Å^3	Block, light red
Z = 4	0.16 × 0.08 × 0.02 mm
$F(000)$ = 1124	

Data collection

XtaLAB Synergy, Dualflex, HyPix diffractometer	T_{min} = 0.689, T_{max} = 1.000
	10492 measured reflections
Radiation source: micro-focus sealed X-ray tube, PhotonJet (Cu) X-ray Source	2289 independent reflections
	2142 reflections with $I > 2\sigma(I)$
Mirror monochromator	R_{int} = 0.023
Detector resolution: 10.0000 pixels mm^{-1}	θ_{max} = 77.9°, θ_{min} = 4.3°
ω scans	h = −16→13
Absorption correction: multi-scan (CrysalisPro; Rigaku OD, 2021)	k = −9→10
	l = −25→24

Refinement

Refinement on F^2	Hydrogen site location: inferred from neighbouring sites
Least-squares matrix: full	
$R[F^2 > 2\sigma(F^2)]$ = 0.027	H-atom parameters constrained
$wR(F^2)$ = 0.084	$w = 1/[\sigma^2(F_o^2) + (0.0583P)^2 + 0.8249P]$
S = 1.10	where $P = (F_o^2 + 2F_c^2)/3$
2289 reflections	$(\Delta/\sigma)_{max}$ = 0.001
126 parameters	$\Delta\rho_{max}$ = 0.38 e Å^{-3}
0 restraints	$\Delta\rho_{min}$ = −0.53 e Å^{-3}
Primary atom site location: dual	

Extinction correction: SHELXL2016/6
(Sheldrick 2015b),
$Fc^* = kFc[1+0.001xFc^2\lambda^3/\sin(2\theta)]^{-1/4}$
Extinction coefficient: 0.00076 (10)

Special details

Geometry. All esds (except the esd in the dihedral angle between two l.s. planes) are estimated using the full covariance matrix. The cell esds are taken into account individually in the estimation of esds in distances, angles and torsion angles; correlations between esds in cell parameters are only used when they are defined by crystal symmetry. An approximate (isotropic) treatment of cell esds is used for estimating esds involving l.s. planes.

Fractional atomic coordinates and isotropic or equivalent isotropic displacement parameters (Å²)

	x	*y*	*z*	U_{iso}*/U_{eq}	Occ. (<1)
Co1	0.500000	0.500000	0.500000	0.02317 (15)	
N1	0.46546 (15)	0.2934 (2)	0.55618 (9)	0.0277 (4)	
C1	0.42663 (16)	0.2229 (3)	0.59925 (10)	0.0261 (4)	
S1	0.37115 (5)	0.12261 (8)	0.65871 (3)	0.03667 (17)	
N11	0.34175 (14)	0.5136 (2)	0.46864 (9)	0.0243 (4)	
C11	0.31849 (16)	0.5744 (3)	0.40943 (11)	0.0258 (4)	
H11	0.371856	0.612144	0.381775	0.031*	
C12	0.21868 (18)	0.5837 (3)	0.38751 (10)	0.0252 (4)	
C13	0.13924 (17)	0.5257 (3)	0.42614 (11)	0.0265 (4)	
H13	0.070717	0.528518	0.411177	0.032*	
C14	0.16372 (18)	0.4638 (3)	0.48723 (12)	0.0271 (4)	
H14	0.111742	0.423819	0.515468	0.033*	
C15	0.26519 (17)	0.4606 (3)	0.50692 (10)	0.0256 (4)	
H15	0.280996	0.419248	0.549211	0.031*	
Br11	0.19160 (2)	0.67390 (3)	0.30387 (2)	0.02899 (12)	
N21	0.53585 (15)	0.3613 (2)	0.41254 (10)	0.0289 (4)	
C21	0.55714 (17)	0.3339 (3)	0.35970 (12)	0.0275 (5)	
C22	0.5843 (2)	0.3030 (3)	0.29171 (13)	0.0364 (5)	
H22A	0.523662	0.315482	0.264145	0.055*	0.5
H22B	0.610963	0.189959	0.287354	0.055*	0.5
H22C	0.636420	0.382640	0.277910	0.055*	0.5
H22D	0.550407	0.384647	0.263646	0.055*	0.5
H22E	0.562352	0.191093	0.279293	0.055*	0.5
H22F	0.658286	0.312341	0.286471	0.055*	0.5

Atomic displacement parameters (Å²)

	U^{11}	U^{22}	U^{33}	U^{12}	U^{13}	U^{23}
Co1	0.0217 (3)	0.0256 (3)	0.0222 (3)	−0.00087 (18)	−0.00012 (17)	0.00064 (18)
N1	0.0256 (9)	0.0280 (9)	0.0294 (9)	−0.0008 (7)	−0.0015 (7)	0.0028 (7)
C1	0.0233 (9)	0.0283 (10)	0.0268 (10)	0.0033 (8)	−0.0026 (8)	−0.0037 (9)
S1	0.0440 (3)	0.0407 (3)	0.0253 (3)	−0.0020 (3)	0.0058 (2)	0.0034 (2)
N11	0.0224 (8)	0.0268 (8)	0.0237 (9)	−0.0009 (7)	−0.0001 (7)	−0.0009 (7)
C11	0.0243 (10)	0.0285 (10)	0.0247 (10)	−0.0022 (8)	0.0002 (8)	−0.0002 (9)
C12	0.0285 (10)	0.0244 (9)	0.0225 (9)	−0.0006 (8)	−0.0011 (8)	−0.0001 (8)

C13	0.0235 (10)	0.0271 (10)	0.0289 (11)	−0.0004 (8)	−0.0001 (8)	0.0000 (8)
C14	0.0235 (10)	0.0285 (10)	0.0293 (10)	−0.0004 (9)	0.0048 (9)	0.0028 (9)
C15	0.0261 (11)	0.0273 (10)	0.0233 (10)	0.0018 (9)	0.0009 (8)	0.0001 (8)
Br11	0.02896 (17)	0.03464 (17)	0.02338 (17)	−0.00212 (9)	−0.00260 (7)	0.00317 (8)
N21	0.0259 (9)	0.0313 (9)	0.0293 (9)	−0.0008 (7)	0.0006 (8)	−0.0004 (8)
C21	0.0251 (10)	0.0270 (10)	0.0305 (12)	−0.0004 (8)	0.0011 (9)	0.0025 (8)
C22	0.0416 (14)	0.0391 (12)	0.0283 (11)	−0.0008 (11)	0.0092 (10)	0.0035 (10)

Geometric parameters (Å, º)

Co1—N1^i	2.0736 (19)	C13—H13	0.9500
Co1—N1	2.0736 (19)	C13—C14	1.383 (3)
Co1—N11	2.1759 (19)	C14—H14	0.9500
Co1—N11^i	2.1758 (19)	C14—C15	1.391 (3)
Co1—N21^i	2.161 (2)	C15—H15	0.9500
Co1—N21	2.161 (2)	N21—C21	1.138 (3)
N1—C1	1.165 (3)	C21—C22	1.457 (3)
C1—S1	1.632 (2)	C22—H22A	0.9800
N11—C11	1.342 (3)	C22—H22B	0.9800
N11—C15	1.343 (3)	C22—H22C	0.9800
C11—H11	0.9500	C22—H22D	0.9800
C11—C12	1.386 (3)	C22—H22E	0.9800
C12—C13	1.389 (3)	C22—H22F	0.9800
C12—Br11	1.892 (2)		
N1^i—Co1—N1	180.0	C13—C12—Br11	120.17 (17)
N1^i—Co1—N11	90.27 (7)	C12—C13—H13	121.3
N1—Co1—N11	89.73 (7)	C14—C13—C12	117.5 (2)
N1—Co1—N11^i	90.27 (7)	C14—C13—H13	121.3
N1^i—Co1—N11^i	89.73 (7)	C13—C14—H14	120.3
N1^i—Co1—N21	84.79 (7)	C13—C14—C15	119.4 (2)
N1—Co1—N21	95.21 (7)	C15—C14—H14	120.3
N1—Co1—N21^i	84.79 (7)	N11—C15—C14	122.8 (2)
N1^i—Co1—N21^i	95.21 (7)	N11—C15—H15	118.6
N11^i—Co1—N11	180.0	C14—C15—H15	118.6
N21^i—Co1—N11^i	89.42 (7)	Co1—N21—C21	160.05 (18)
N21^i—Co1—N11	90.59 (7)	N21—C21—C22	178.7 (2)
N21—Co1—N11	89.41 (7)	C21—C22—H22A	109.5
N21—Co1—N11^i	90.58 (7)	C21—C22—H22B	109.5
N21—Co1—N21^i	180.00 (6)	C21—C22—H22C	109.5
Co1—N1—C1	154.96 (18)	C21—C22—H22D	109.5
N1—C1—S1	179.1 (2)	C21—C22—H22E	109.5
C11—N11—Co1	120.11 (14)	C21—C22—H22F	109.5
C11—N11—C15	118.17 (19)	H22A—C22—H22B	109.5
C15—N11—Co1	121.72 (15)	H22A—C22—H22C	109.5
N11—C11—H11	119.1	H22B—C22—H22C	109.5
N11—C11—C12	121.8 (2)	H22D—C22—H22E	109.5
C12—C11—H11	119.1	H22D—C22—H22F	109.5

| C11—C12—C13 | 120.5 (2) | H22E—C22—H22F | 109.5 |
| C11—C12—Br11 | 119.37 (17) | | |

Symmetry code: (i) −x+1, −y+1, −z+1.

Hydrogen-bond geometry (Å, º)

D—H···A	D—H	H···A	D···A	D—H···A
C11—H11···N1ⁱ	0.95	2.60	3.109 (3)	114
C15—H15···N1	0.95	2.63	3.121 (3)	113
C22—H22*A*···S1ⁱⁱ	0.98	2.98	3.947 (3)	168
C22—H22*B*···S1ⁱⁱⁱ	0.98	2.76	3.625 (3)	147
C22—H22*C*···Br11ⁱᵛ	0.98	2.97	3.840 (3)	148
C22—H22*F*···Br11ᵛ	0.98	2.92	3.681 (3)	135

Symmetry codes: (i) −x+1, −y+1, −z+1; (ii) x, −y+1/2, z−1/2; (iii) −x+1, −y, −z+1; (iv) x+1/2, y, −z+1/2; (v) −x+1, y−1/2, −z+1/2.